Journal of Child Neurology
2015, Vol. 30(10) 1343-1348

DOI: 10.1177/0883073814562252
jcn.sagepub.com
SAGE

Early-Onset Aicardi-Goutières Syndrome: Magnetic Resonance Imaging (MRI) Pattern Recognition

Adeline Vanderver, MD[1,2], Morgan Prust, BS[3], Nadja Kadom, MD[4], Scott Demarest, MD[2], Yanick J. Crow, BMedSci, MBBS, MRCP, PhD[5,6], Guy Helman, BS[2], Simona Orcesi, MD[7], Roberta La Piana, MD[8], Carla Uggetti, MD[9], Jichuan Wang, PhD[10], Heather Gordisch-Dressman, PhD[10], Marjo S. van der Knaap, MD, PhD[11], and John H. Livingston, MBCHB, FRCP, FRCPCH[12]

Abstract

Aicardi-Goutières syndrome is an inherited leukodystrophy with calcifying microangiopathy and abnormal central nervous system myelination. As fewer diagnostic computed tomographic (CT) scans are being performed due to increased availability of magnetic resonance imaging (MRI), there is a potential for missed diagnoses on the basis of calcifications. We review a series of patients with MRIs selected from IRB-approved leukodystrophy biorepositories to identify MRI patterns for recognition of early-onset Aicardi-Goutières syndrome and scored for a panel of radiologic predictors. Each individual predictor was tested against disease status using exact logistic regression. Features for pattern recognition of Aicardi-Goutières syndrome are temporal lobe swelling followed by atrophy with temporal horn dilatation, early global cerebral atrophy and visible calcifications, as evidenced by 94.44% of cases of Aicardi-Goutières syndrome correctly classified with a sensitivity of 90.9% and specificity of 96.9%. We identify a panel of MRI features predictive of Aicardi-Goutières syndrome in young patients that would differentiate it from other leukoencephalopathies.

Keywords

pediatric neuroradiology, leukodystrophies, Aicardi-Goutières syndrome

Received June 17, 2014. Received revised September 09, 2014. Accepted for publication November 07, 2014.

Aicardi-Goutières syndrome is an inherited leukoencephalopathy caused by mutations in *TREX1*,[1] *SAMHD1*,[2] *RNASEH2A*, *RNASEH2B* and *RNASEH2C*,[3] *ADAR1*,[4] and *IFIH1*.[5] These genes, when mutated, are believed to cause an accumulation of immune stimulatory nucleic acids and activation of innate cellular immunity, resulting in the characteristic phenotype of cerebrospinal

[1] Center for Genetic Medicine Research, Children's National Health System Washington, DC, USA
[2] Department of Neurology, Children's National Health System, Washington, DC, USA
[3] Harvard Medical School, Harvard University, Boston, MA, USA
[4] Department of Radiology, Children's National Health System, Washington, DC, USA
[5] Manchester Academic Health Science Centre, University of Manchester, Genetic Medicine, Manchester, United Kingdom
[6] Department of Genetics, INSERM U781, Université Paris Descartes- Sorbonne Paris Cité, Institut Imagine, Hôpital Necker Enfants Malades (AP-HP), Paris, France
[7] Child Neurology and Psychiatry Unit, C. Mondino National Neurological Institute, Pavia, Italy
[8] Department of Neuroradiology, Montreal Neurological Institute and Hospital, McGill University, Montreal, Quebec, Canada
[9] Unit of Neuroradiology, Department of Radiology, San Carlo Borromeo Hospital, Milano, Italy
[10] Department of Biostatistics, Children's National Health System, Washington, DC, USA
[11] Department of Child Neurology, VU University Medical Center, Amsterdam, the Netherlands
[12] Department of Paediatric Neurology, Leeds Teaching Hospitals NHS Trust, Leeds, United Kingdom

Corresponding Author:
Adeline Vanderver, MD, Department of Neurology, Children's National Health System, 111, Michigan Avenue, NW, Washington, DC 20010, USA.
Email: avanderv@childrensnational.org

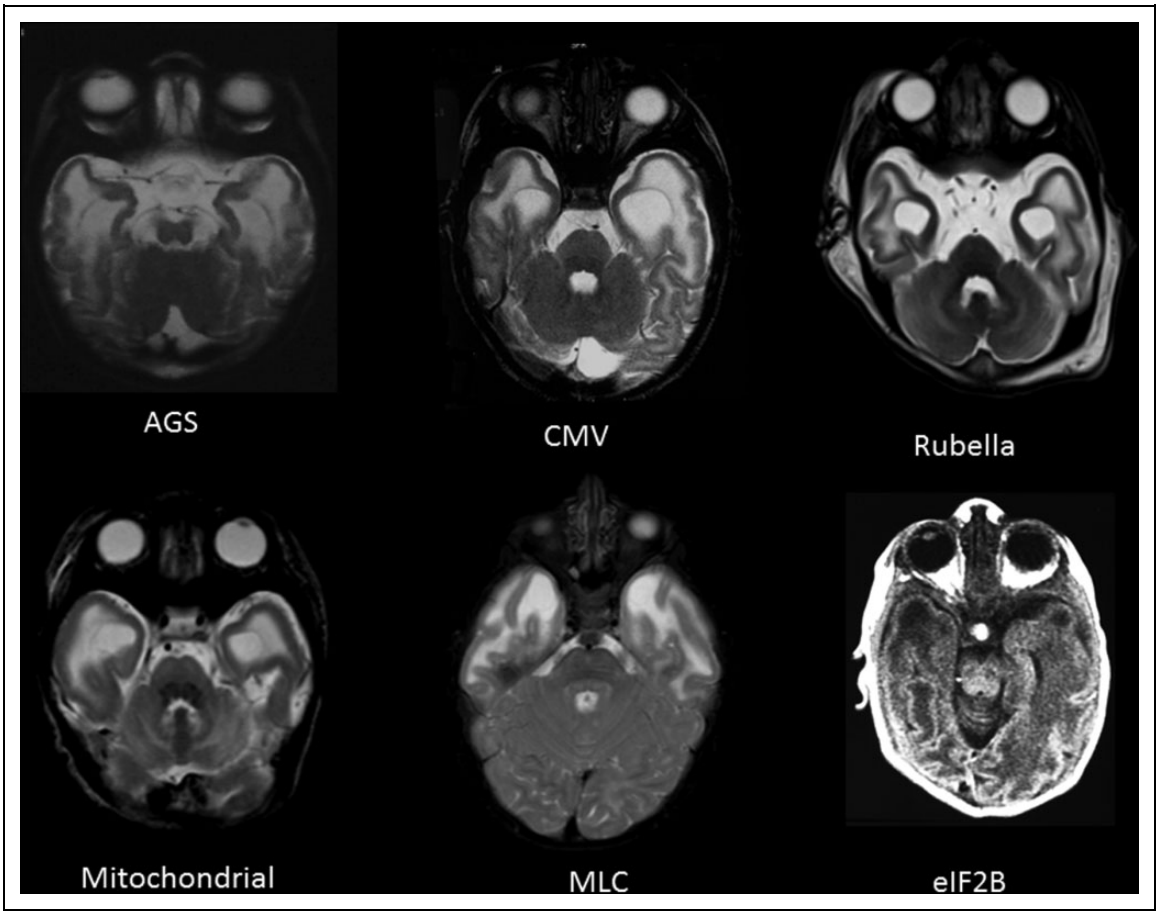

Figure 1. Swollen temporal lobes on MRI may have many causes, including a few depicted here: Aicardi-Goutières syndrome (AGS), congenital infection with cytomegalovirus (CMV) or rubella, mitochondrial leukoencephalopathies, megalencephalic leukoencephalopathy with subcortical cysts (MLC), and antenatal-onset vanishing white matter with *eIF2B* mutations. In addition, reported cases include cystic leukoencephalopathy without megalencephaly due to *RNASET2* mutations and various types of congenital muscular dystrophies (Fukuyama congenital muscular dystrophy [FCMD], Walker-Warburg syndrome, and congenital muscular dystrophy type 1D [MDC1D]).

fluid pleocytosis, increased cerebrospinal fluid alpha interferon, and a calcifying microangiopathy with abnormal central nervous system white matter.[6] Classically, this diagnosis is suspected when typical calcifications are identified on computed tomographic (CT) imaging in the appropriate clinical context.

Because of the increased availability of magnetic resonance imaging (MRI) and to concerns with exposure to radiation, fewer CT scans are now performed as part of a diagnostic evaluation. This may result in missed opportunities to diagnose Aicardi-Goutières syndrome, unless characteristic MRI patterns are identified that permit suspicion of the disorder and appropriate diagnostic testing. In addition, patients without calcifications at disease onset have been identified[7-10] so that a lack of cerebral calcifications cannot be considered an exclusionary criterion.[7,11,12]

For these reasons, it is important to explore the diagnostic utility of MRI in Aicardi-Goutières syndrome, in particular in early-onset cases in the first year of life. In addition to intracranial calcifications, Aicardi-Goutières syndrome has been associated with abnormal cerebral white matter and cerebral atrophy.[11-16] White matter abnormalities may be either diffuse or with an anteroposterior gradient, including a swollen appearance of anterior frontal and anterior temporal gyri.[7,17] Younger patients and patients with the anteroposterior gradient were also likely to have frontotemporal cysts as additional features.[7] Finally, early-onset atrophy is also a prominent finding in a majority of Aicardi-Goutières syndrome patients,[7] and it may be progressive, involving the entire cerebral hemispheres[7] and brainstem,[18] with relative cerebellar sparing.[7]

Differential diagnosis of the combination of calcification, atrophy, and swollen frontal or temporal white matter with or without cysts is particularly challenging in the first 2 years of life, as these may be seen in a number of early-onset disorders of the white matter (Figure 1). These include acquired white matter diseases, such as congenital infections (eg, cytomegalovirus or rubella). Additionally, certain inherited disorders of the white matter, or leukodystrophies, can demonstrate overlapping radiologic findings. These include Alexander disease (presence of cysts and frontal predominance), megalencephalic leukoencephalopathy with subcortical cysts (prominent temporal involvement and cysts), vanishing white matter disease (rarefaction of white matter, temporal cysts in severe variants),

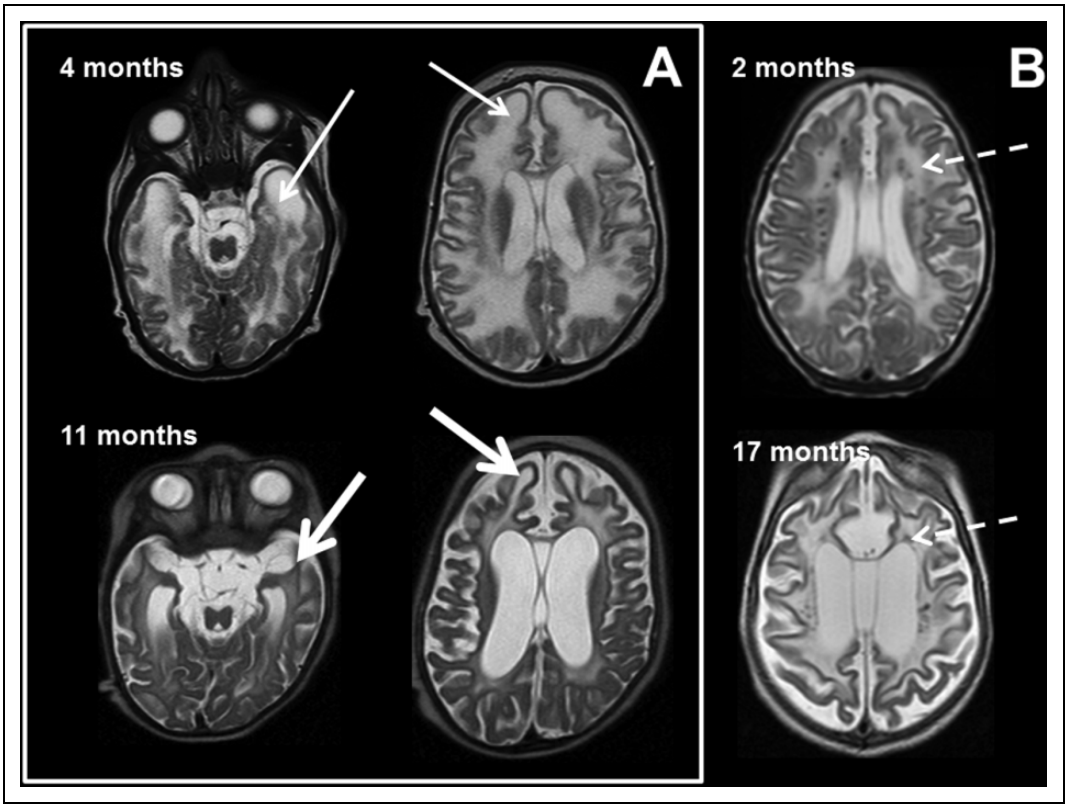

Figure 2. MRI characteristics in Aicardi-Goutières syndrome: MRI obtained in 2 patients with Aicardi-Goutières syndrome at ages 4 months (upper row) and 11 months (lower row) in A and the second patient with images at 2 and 17 months in B. The images demonstrate early frontal and temporal lobe swelling (thin white arrow) that gives way to severe frontal and temporal lobe atrophy (thick white arrows), as well as the prominent global atrophy. Note also the T_2 dark signal abnormalities presumed to be calcifications present at 2 months and present at 17 months in the second patient (dashed arrows).

ribonuclease T2 (RNaseT2)-related disease (temporal lobe cysts), rubella, mitochondrial leukoencephalopathies (temporal lobe involvement), various types of congenital muscular dystrophies (Fukuyama congenital muscular dystrophy, Walker-Warburg syndrome, congenital muscular dystrophy type 1D) (temporal lobe involvement), and leukoencephalopathy with calcifications and cysts (cysts and calcifications).

We sought to identify a panel of MRI features predictive of Aicardi-Goutières syndrome in very young patients that would differentiate it from other white matter diseases that present with similar radiologic features and permit the clinician to order appropriate diagnostic testing.

Methods

Standard Protocol Approvals, Registrations, and Patient Consents

MRI images of patients with mutation-proven Aicardi-Goutières syndrome (AGS; n = 23, including AGS1, n = 14; AGS2 = 3, AGS3 = 3, AGS5 = 3), infantile Alexander disease (n = 9), megalencephalic leukoencephalopathy with subcortical cysts (n = 5), congenital cytomegalovirus infection (n = 4), leukoencephalopathy with calcifications and cysts (n = 3), and vanishing white matter disease (n = 9) were reviewed according to a standard protocol. Imaging studies from patients with proven leukodystrophies with infantile-onset were selected. Age at first MRI and basic clinical information was recorded. All patients were selected from an institutional review board (IRB)–approved biorepository of leukodystrophy subjects collected from clinical centers with expertise in these disorders. Informed consent was obtained from all the patients evaluated at Children's National Health System and the University of Manchester.

Radiologic Criteria

All MRIs were scored for a series of radiologic predictors, including cerebral, cerebellar, and brainstem atrophy; location of white matter abnormalities; presence within abnormal white matter of regions of hypointense T_2 signal or hyperintense T_1 signal suggesting areas of more normal myelin development or mineralization; more hyperintense T_2 signal in an irregular fashion in subcortical regions; evidence of white matter rarefaction on fluid-attenuated inversion recovery imaging, visibility of calcifications on standard T_1 and T_2 imaging (as confirmed with correlation by CT scan review) on MRI; basal ganglia signal abnormalities and atrophy; cystic changes within brain parenchyma; and the finding of swelling or focal atrophy of areas including the frontal or temporal lobes (Figure 2). MRIs were scored by a pediatric neuroradiologist (NK) who was blinded to the patient's diagnosis.

Statistical Analysis

Each individual predictor was tested against disease status (Aicardi-Goutières syndrome vs non–Aicardi-Goutières syndrome) using exact

Table 1. Testing Each Predictor Against Disease Status.

Predictor	OR	95% CI	*P* value
Cerebral atrophy	25.65	6.08-108.24	<.0001
Brain stem atrophy or hypoplasia	25.67	4.96-132.94	<.0001
Cerebral WM loss/ventricular dilation	36.67	4.37-307.92	.001
Irregular high signal T_2 in cerebral subcortical region	13.56	1.53-120.03	.019
Anterior >posterior gradient on T_1 or T_2	7.92	2.29-27.40	.001
Low signal T_2 in WM	0.25	0.08-0.78	.019
Calcification on MR	19.44	4.91-76.93	<.0001
Cerebellar WM abnormal	1.66	0.56-4.96	.364
Basal ganglia signal abnormal	1.47	0.50-4.33	.481
Basal ganglia atrophy	6.42	1.70-24.24	.006
Corpus callosum thin	5.50	0.61-49.37	.128
Cysts, nontemporal	3.27	1.01-10.56	.047
Temporal horn dilation	14.73	3.88-55.99	<.0001
Frontal gyri swelling	2.08	0.70-6.23	.190
Frontal atrophy	11.54	2.21-60.19	.004
Swollen temporal pole	5.26	1.56-17.76	.007
Temporal atrophy	33.82	3.93-291.15	.001
Midparietal swollen gyri	1.93	0.61-6.14	.266

Abbreviations: CI, confidence interval; MR, magnetic resonance; OR, odds ratio; WM, white matter.

logistic regression. All predictors with a *P* value less than .05 were compared pairwise to determine which predictors exhibit collinearity. Unique predictors having a significant relationship with disease status were included in a stepwise logistic regression model (probability criteria for exclusion/inclusion set to 0.2). All predictors entered into the model had equal chance of retention/exclusion at each step. The final model was developed by combining results from the stepwise process and iteratively including/excluding predictors felt to be most clinically relevant while accessing model fit via the Bayesian information criterion. Odds ratios, *P* values, and 95% confidence intervals are reported for those predictors surviving the selection process. A classification table was prepared for this final model.

Results

All proposed predictors appeared individually statistically predictive of Aicardi-Goutières syndrome, with the exception of a thin corpus callosum, signal abnormalities in the basal ganglia and cerebellar white matter, and swollen-appearing white matter in the parietal regions. Exact logistic regression analysis of each variable against diagnosis of Aicardi-Goutières syndrome identified 13 variables with *P* values <.05 (Table 1). However, multiple-variable logistic regression analysis identified a combined model that included only a few of these features (Table 2). This correctly identified 94.44% of cases of Aicardi-Goutières syndrome present in this sample (sensitivity 90.91%, specificity 96.88%, positive predictive value 95.24%, negative predictive value 93.94%). These results were used in preparation of a diagnostic algorithm based on the proposed predictors of Aicardi-Goutières syndrome based on the retained clinical predictors (Figure 3).

Patient's ages were a mean 1.2 years, median 0.7 year, whereas controls were a mean 3.4 years, median 2.2 years. All patients whose data were available in both the Aicardi-Goutières syndrome and control groups were developmentally delayed early in their clinical presentations: 23/23 (100%) of Aicardi-Goutières syndrome cases and 23/23 (100%) of control cases. There was a higher frequency of gastrostomy tube feeding dependence in the Aicardi-Goutières syndrome population (11/16 where data were available or 69%) versus the control population (5/19 where data were available or 26%) (Supplementary Data Table 1 is available at http://jcn.sagepub.com/supplemental). Similarly, fewer of the Aicardi-Goutières syndrome patients than controls were ambulatory or verbal, though this may be in part a reflection of their younger age. Exact logistic regression was used in this analysis because of a small sample size.

Discussion

This approach develops an algorithm for early onset leukodystrophies, to aid in the analysis of MRIs felt to be possibly consistent with Aicardi-Goutières syndrome. The combination of temporal lobe swelling or temporal horn dilation, with progressive atrophy, in particular of the frontal lobe, appears fairly specific of Aicardi-Goutières syndrome. Also notable was the fact that when carefully sought, calcifications were often visible on standard T_1 and T_2 MRI images, and when identified were highly specific for Aicardi-Goutières syndrome. Together, these features can help suggest a diagnosis of Aicardi-Goutières syndrome, and can be used by the clinician to determine the need for a CT scan or specific MRI modalities to identify calcifications and may prompt molecular or biochemical testing.

It is important to note that this algorithm was developed from leukoencephalopathies with features that could be overlapping with Aicardi-Goutières syndrome, such as a temporal or frontal predominance of leukoencephalopathy or presence of calcifications, and still needs to be validated in a larger cohort of unsolved leukodystrophies. Additionally, this model is developed from and for patients with early-onset leukoencephalopathies and may not be pertinent in Aicardi-Goutières syndrome patients with later age of onset.[7]

Additional limitations of the study included lack of perfect age matching of the samples. This is a reflection of the fact that these diseases have slightly different typical ages of onset, and therefore slightly different ages of available MRI studies. Also of note, a predominance of patients with Aicardi-Goutières syndrome in this study had mutations in *TREX1*, and patients with mutations in the other genes were underrepresented. This is in part determined by the fact that cases were selected based on early age at onset, and first imaging. Patients with *TREX1* mutations are more likely to have an earlier onset and we cannot definitely exclude that the observed results—that is, the specificity of temporal pole swelling and cystic degeneration—reflect the peculiar distribution of the mutated genes in our sample.

Finally, as is often the case in rare disease research, our small sample size limited the range of feasible statistical

Table 2. Best Fit Model.

Predictor	OR	SE	OR 95% CI	Coefficient	*P* value
Swollen temporal pole	25.25	37.70	1.35-471.09	3.229	.032
Temporal horn dilation	40.35	58.79	2.32-701.66	3.698	.011
Calcification visible on MRI	14.99	19.71	1.14-197.23	2.707	.039
Cerebral atrophy	86.17	138.51	3.69-2012.04	4.456	.006

Abbreviations: CI, confidence interval; MRI, magnetic resonance imaging; OR, odds ratio; SE, standard error.

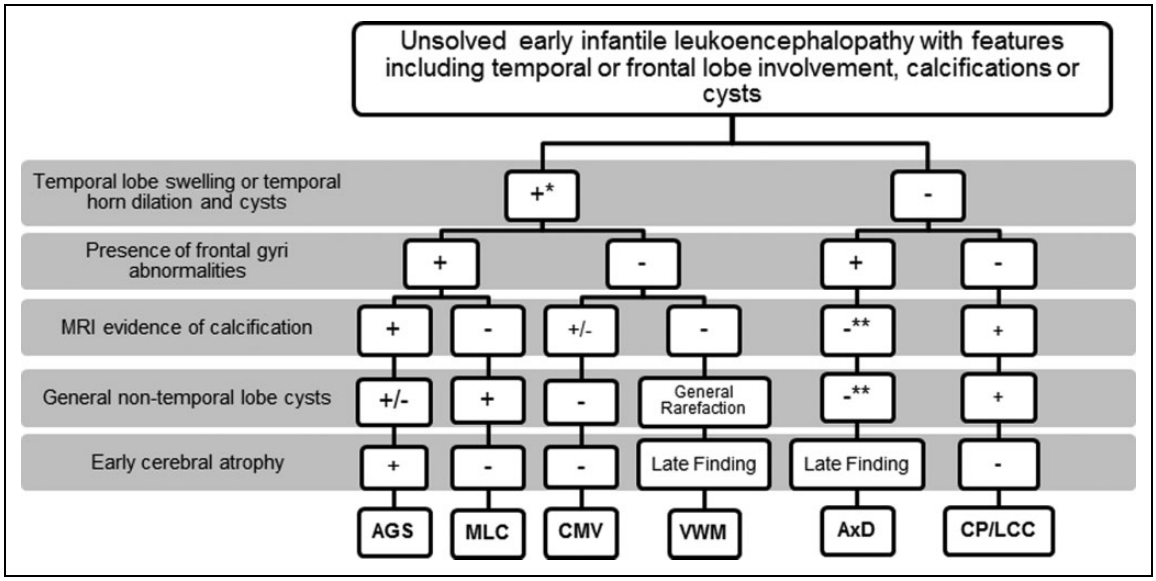

Figure 3. MRI characteristics of unsolved early-infantile leukoencephalopathy. MRI analyses were used to identify a possible descriptive algorithm of features on MRI consistent with the diagnosis of Aicardi-Goutières syndrome (AGS). Features of radiologic findings from megalencephalic leukoencephalopathy with subcortical cysts (MLC), cytomegalovirus (CMV), vanishing white matter disease (VWM), Alexander disease (AxD), and Coats plus disease/leukoencephalopathy with calcifications and cysts (CP/LCC) are depicted. Note the features of temporal lobe swelling followed by atrophy with temporal horn dilatation, early global cerebral atrophy, and visible calcifications on MRI in young patients with Aicardi-Goutières syndrome. This appears to be a promising group of features for pattern recognition on MRI. *Temporal lobe swelling occurs in early infantile cases of vanishing white matter disease, whereas it is not an MRI feature found in late-onset vanishing white matter disease patients. In addition, early infantile cases frequently have anterior temporal cysts. **Indicates a generally rare feature but exceptions have been found.

analyses. In order to decrease the risk of statistical overfitting, where the developed model is only applicable to the sample at hand and not generalizable to the population, we took an iterative approach where we evaluated each predictor and the effect of a combination of predictors to arrive at a model that balances fit to the data with generalizability. Despite the high quality of fit, our results were based on only 23 Aicardi-Goutières syndrome patients and 30 non–Aicardi-Goutières syndrome control subjects as evidenced by the very wide confidence intervals. As the number of leukoencephalopathies with similar MRI features are discovered and additional patients are found and included in the analysis, the results presented here may change.

Additionally, although a number of other disorders may have overlapping radiologic features with Aicardi-Goutières syndrome, such as temporal or frontal lobe predominance, calcifications, and cysts, these typically have other characteristics that may permit pattern recognition. These non–Aicardi-Goutières syndrome relevant MRI characteristics were not scored, as our small sample size precluded the statistical analysis of a larger set of variables. For example, these include, in Alexander disease, findings of basal ganglia and brainstem findings as well as the extensive contrast enhancement; in megalencephalic leukoencephalopathy with subcortical cysts, persistently swollen gyri and late atrophy with sometimes extensive cysts; in vanishing white matter disease, significant rarefaction of affected white matter; and in leukoencephalopathy with calcifications and cysts, the globular nature of calcifications in large aggregates and the large intraparenchymal cysts.

The proposed algorithm therefore does not take into consideration the full complexity of recognizing a likely diagnosis in an individual MRI. The entire constellation of clinical and radiologic features should be appreciated in each patient during diagnostic workup. However, features of temporal lobe swelling followed by atrophy with temporal horn dilation, early global cerebral atrophy, and visible calcifications on MRI appears

to be a promising group of features for pattern recognition on MRI in young patients with Aicardi-Goutières syndrome. These features may help a clinician recognize Aicardi-Goutières syndrome in an era where CT scans are less often performed, and there is a greater potential for missing the pathognomonic calcifications seen in this disorder.

These diagnostic imaging markers present a phenotype that is useful in evaluating MRI features in the diagnosis of early Aicardi-Goutières syndrome versus other early-onset leukodystrophies, further validating previous descriptions of this early-onset Aicardi-Goutières syndrome phenotype.[7,19]

Acknowledgments

The authors thank the families of the patients included in this study, as well as the Myelin Disorders Bioregistry Project. We thank Luca Ramenghi for images of a patient with congenital rubella and Dr Raphael Schiffman for contributing patients.

Author Contributions

AV, YC, JL, and MSK managed the project. NK, RLP, CU, SD, SM, MSK, JL, YC, and AV performed MRI examination. HGD and JW designed the statistical analyses. AV and HGD performed the data analyses. MP, SD, GH, YC, JL, MSK, and AV wrote the paper.

Declaration of Conflicting Interests

The authors declared the following potential conflicts of interest with respect to the research, authorship, and/or publication of this article: AV provides unpaid consulting to StemCells Inc.

Funding

The authors disclosed receipt of the following financial support for the research, authorship, and/or publication of this article: This study was partially funded by the European Union's Seventh Framework Programme (FP7/2007-2013) under grant agreement 241779, a European Research Council (GA 309449) grant to YJC. The participation of MP and GH was supported by the Delman fund and the Neurogenetics Program at Children's National Health System. AV's involvement was supported by a K08 from NINDS.

References

1. Crow YJ, Hayward BE, Parmar R, et al. Mutations in the gene encoding the 3′-5′ DNA exonuclease TREX1 cause Aicardi-Goutieres syndrome at the AGS1 locus. *Nat Genet*. 2006;38: 917-920.
2. Rice GI, Bond J, Asipu A, et al. Mutations involved in Aicardi-Goutieres syndrome implicate SAMHD1 as regulator of the innate immune response. *Nat Genet*. 2009;41:829-832.
3. Crow YJ, Leitch A, Hayward BE, et al. Mutations in genes encoding ribonuclease H2 subunits cause Aicardi-Goutieres syndrome and mimic congenital viral brain infection. *Nat Genet*. 2006;38:910-916.
4. Rice GI, Kasher PR, Forte GM, et al. Mutations in ADAR1 cause Aicardi-Goutieres syndrome associated with a type I interferon signature. *Nat Genet*. 2012;44:1243-1248.
5. Rice GI, Del Toro Duany Y, Jenkinson EM, et al. Gain-of-function mutations in IFIH1 cause a spectrum of human disease phenotypes associated with upregulated type I interferon signaling. *Nat Genet*. 2014;46:503-509.
6. Goutieres F, Aicardi J. Acute neurological dysfunction associated with destructive lesions of the basal ganglia in children. *Ann Neurol*. 1982;12: 328-332.
7. Uggetti C, La Piana R, Orcesi S, Egitto MG, Crow YJ, Fazzi E. Aicardi-Goutieres syndrome: neuroradiologic findings and follow-up. *AJNR Am J Neuroradiol*. 2009;30:1971-1976.
8. Aicardi J, Goutières F. A progressive familial encephalopathy in infancy with calcifications of the basal ganglia and chronic cerebrospinal fluid lymphocytosis. *Ann Neurol*. 1984;15: 49-54.
9. D'Arrigo S, Riva D, Bulgheroni S, et al. Aicardi-Goutières syndrome: description of a late onset case. *Dev Med Child Neurol*. 2008;50:631-634.
10. Goutieres F, Aicardi J, Barth PG, Lebon P. Aicardi-Goutieres syndrome: an update and results of interferon-alpha studies. *Ann Neurol*. 1998;44:900-907.
11. Crow YJ, Livingston JH. Aicardi-Goutieres syndrome: an important Mendelian mimic of congenital infection. *Dev Med Child Neurol*. 2008;50:410-416.
12. Orcesi S, La Piana R, Fazzi E. Aicardi-Goutieres syndrome. *Br Med Bull*. 2009;89:183-201.
13. Goutieres F. Aicardi-Goutieres syndrome. *Brain Dev*. 2005;27: 201-206.
14. Lanzi G, Fazzi E, D'Arrigo S. Aicardi-Goutieres syndrome: a description of 21 new cases and a comparison with the literature. *Eur J Paediatr Neurol*. 2002;6(suppl A):A9-A22; discussion A3-A5, A77-A86.
15. Lanzi G, Fazzi E, D'Arrigo S, et al. The natural history of Aicardi-Goutieres syndrome: follow-up of 11 Italian patients. *Neurology*. 2005;64:1621-1624.
16. Ostergaard JR, Christensen T. Aicardi-Goutieres syndrome: neuroradiological findings after nine years of follow-up. *Eur J Paediatr Neurol*. 2004;8: 243-246.
17. Van der Knaap M. *Magnetic Resonance of Myelination and Myelin Disorders*. 3rd ed. Berlin: Springer-Verlag; 2005: 284-342.
18. Crow YJ, Massey RF, Innes JR, et al. Congenital glaucoma and brain stem atrophy as features of Aicardi–Goutières syndrome. *Am J Med Genet A*. 2004;129A:303-307.
19. van der Knaap M, Valk J. *Magnetic Resonance of Myelination and Myelin Disorders*. 3rd ed. Berlin, Germany: Springer; 2005.